



## Design and prototyping of a low-cost vehicle localization system with guaranteed convergence properties

Silvère Bonnabel<sup>a</sup>, Erwan Salaün<sup>b,\*</sup>

<sup>a</sup> Centre de Robotique, Mines ParisTech, 60 boulevard Saint-Michel, 75272 Paris Cedex 06, France

<sup>b</sup> School of Aerospace Engineering, Georgia Institute of Technology, Atlanta, GA 30332-0150, USA

### ARTICLE INFO

#### Article history:

Received 12 March 2010

Accepted 15 February 2011

Available online 16 March 2011

#### Keywords:

Low-cost vehicle localization system

Nonlinear filter

Nonholonomic constraints

Guaranteed convergence properties

Symmetries

### ABSTRACT

This work presents a low-cost vehicle localization system, using measurements from one gyroscope, two wheel speed sensors and a GPS, to estimate the heading, velocity and position of a vehicle. Taking advantage of the nonholonomic constraints, the design of the observer (or “filter”) takes into account imperfections of the embedded sensor measurements, such as a slowly time-varying gyroscope bias or some uncertainty in the wheel diameter value. Thanks to a well-chosen nonlinear structure, the estimator is easy to tune, easy to implement, and well-behaved even at very low speed. Moreover, the proposed filter has guaranteed convergence properties when GPS is available and keeps providing good estimations during GPS losses. Simulation and experiment results in urban area illustrate the good performance of the algorithm.

© 2011 Elsevier Ltd. All rights reserved.

### 1. Introduction

The vehicle localization problem has been a field of extensive research over the past 20 years, for military and civil purposes. Recent applications of embedded localization systems, which are able to accurately estimate the vehicle position, velocity, and orientation, involve generating precise urban maps (e.g. Google Streetview, 3D environmental maps from mobile mapping systems), the use of floats of vehicles, such as buses and taxis, to update these maps, and the growing development of semi or fully automatic vehicle control systems. The global position system (GPS) has become a widespread device that is used in most of vehicle localization system (VLS) algorithms. It provides estimations of the vehicle position and velocity in an inertial frame. In normal conditions, standard commercial GPS have a (only) relative accuracy (approximately 2 m circular error of probability in position estimation) and low update rate (1–4 Hz). Moreover, lack of GPS is very common in urban environments (or on country roads surrounded by vegetation). Indeed in the so-called urban canyons, the buildings tend to either mask the GPS transmitted signal, or to reflect it along multipaths, or to gather the visible satellites in a tiny solid angle (increasing estimation errors). Such configurations can lead to excessively degraded GPS signal

outputs. Moreover, in indoors environments, or tunnels, GPS is totally unavailable.

For all those reasons, the localization task is generally assigned to embedded sensors which are “aided” by GPS: the sensors drifts are corrected thanks to the GPS estimations, which are, in the long run, accurate on average. Such VLS allow to improve GPS estimations, even in wide-open environments. Recent technological developments of low-cost embedded sensors, especially micro-electro-mechanical systems (MEMS), have been a major factor in the development of such GPS-aided VLS. In addition to GPS, numerous on-board system design have then been proposed: Davidson, Hautamäki, and Collin (2008) and Bevely (2004) use inertial measurement unit (IMU, i.e. accelerometers and gyroscopes), Zhang, Gu, Milios, and Huynh (2005) use IMU and digital compass, Dissanayake, Sukkarieh, Nebot, and Durrant-Whyte (2001) and Di Domenico, Fiengo, and Glielmo (2007) use IMU and speedometers (wheel speed sensors), Hohman, Murdock, Westerfield, Hattox, and Kusterer (2000) use IMU and differential GPS.

The VLS rely then on the fusion of the several sensors measurements and a trusted model of the vehicle dynamics. The trusted dynamical model can be entirely based on general kinematic equations, considering the system as a material point to which a frame is attached (orientation of the vehicle). In this case, any algorithm designed for any moving system (e.g. an aerial vehicle) may be used (e.g. see Martin & Salaün, 2008a, 2008b; Vasconcelos, Silvestre, & Oliveira, 2008; Zhang et al., 2005; or any commercial off-the-shelf system, often called “aided attitude and heading reference systems” (aided AHRS), e.g. MIDG II from Microbotics, or MTi-G from Xsens). However, a specific

\* Corresponding author.

E-mail addresses: [silvere.bonnabel@mines-paristech.fr](mailto:silvere.bonnabel@mines-paristech.fr) (S. Bonnabel), [erwan.salaun@gatech.edu](mailto:erwan.salaun@gatech.edu) (E. Salaün).

model of terrestrial vehicles may improve the estimation performances. In particular, [Dissanayake et al. \(2001\)](#) have shown that considering nonholonomic constraints significantly improves the precision of the VLS. This kind of roll without slip model has been advocated in several recent publications such as [Fiengo, Di Domenico, and Glielmo \(2009\)](#) and [Di Domenico et al. \(2007\)](#).

The data fusion between the trusted dynamical model, and the several sensors measurements generally relies on standard filtering methods, such as Luenberger observer, Extended or Unscented Kalman Filter (e.g. see [Bevly, Ryu, & Gerdes, 2006](#); [Fiengo et al., 2009](#); [Ryu & Gerdes, 2004](#), or [Sebsadji, Glaser, Mammari, & Dakhallallah, 2008](#) that combines both methods), which yield remarkably good results when properly tuned and implemented. Nevertheless, these techniques suffer several drawbacks: it is not easy to choose the numerous parameters of the filter (the design principally relies on extensive simulations); it is not easy to implement the filter (skills in real-time implementation are required to handle the numerous matrix operations); the filter is computationally expensive and needs an expensive computation board to run the algorithm in real-time.

Another main drawback of the popular filtering techniques is that the models involved are nonlinear, so it is in general very difficult to prove the convergence of the estimation error to zero, even on the first order expansion of the error around any trajectory, since the linearized error equation is time-varying. If the system is badly initialized, or if the estimation differs much from the true state value after a long GPS loss (e.g. in a tunnel), there is absolutely no theoretical guarantee that the filter behaves well, i.e. the estimation error converges to zero. To circumvent this problem, some recent work have aimed at developing nonlinear observers with guaranteed convergence properties (e.g. see [Grip et al., 2008](#); [Imsland et al., 2006](#) who have developed nonlinear observers for lateral velocity estimation using an accurate road friction model, see also [Bonnabel, Martin, & Rouchon, 2008, 2009](#); [Lageman, Mahony, & Trumppf, 2008](#); [Lageman, Trumppf, & Mahony, 2010](#)).

In this paper, a low-cost vehicle localization system with guaranteed convergence properties is proposed. It merges measurements from one low-cost gyroscope, two wheel speed sensors and a GPS. Based on the nonholonomic constraints of the vehicle, the observer design takes also into account sensor imperfections such as slowly time-varying gyroscope bias and wheel diameter. Indeed, contrary to high-precision expensive gyroscope that have a very stable in time bias, (that can then be estimated at rest), the bias of low-cost gyroscope is very sensitive to exterior parameters (e.g. temperature) and has a trend to slowly drift. If this bias is not continuously estimated online, it can yield inaccurate estimates of the vehicle state (as shown in [Martin & Salaün, 2008b](#)). An online estimation of the gyro bias (and uncertainty in wheel radius value) allows the estimator to provide accurate estimation during relatively long GPS losses.

In addition to its convergence properties, the proposed filtering algorithm is easy to tune (only four parameters to choose), easy to implement and computationally economic (very few scalar operations), with a nice cascade structure; and the gains of the observer automatically adapt to the speed of the car. Last, but not least, no division by terms corresponding to sensors measurements is ever required. Indeed, such division may have a dramatic effect at low speed. One major drawback of usual VLS filtering strategy is the estimation of the yaw angle that is very often based on the *arctan* of the ratio between GPS velocity measurements. As demonstrated in [Bevly \(2004\)](#), this technique leads to very poor results at low speed due to GPS measurements noise: it is then usual to define a threshold in the norm of the velocity (typically 2 m/s) under which the estimated yaw angle is not corrected anymore, see [Davidson et al. \(2008\)](#). The algorithm

presented in this paper bypasses this limitation and keeps providing good estimations at very low speed.

To sum up, the main contribution of this article is to propose a simple easy-to-tune nonlinear observer for VLS, which takes into account several sensor measurement imperfections. It can be seen as a credible alternative to Kalman-based filtering algorithms usually used for vehicle localization. Beyond several nice features, the main advantage of the proposed observer is that it has guaranteed convergence properties for a very large set of trajectories (although the system is nonlinear and time-varying). Such theoretical guarantees allow the observer to be robust to GPS losses, and from an industrial viewpoint, it can be of great interest for safety, especially if the estimator is used for feedback control of vehicle.

The structure of the proposed observer is based on the recent theory of “symmetry-preserving observers”, introduced in [Bonnabel et al. \(2008, 2009\)](#), which allowed to design nonlinear filters for AHRS and aided AHRS with strong theoretical and practical properties (see [Martin & Salaün, 2007, 2010](#) for AHRS and [Martin & Salaün, 2008a, 2008b](#) for aided AHRS). Preliminary theoretical results regarding VLS and symmetry-preserving observers can be found in [Guillaume and Rouchon \(1998\)](#) and [Bonnabel et al. \(2008\)](#).

This paper is organized as follows. In Section 2, the system model is first described, taking into account nonholonomic constraints of the vehicle and imperfections of the low-cost embedded sensors (gyro bias and unknown wheel radius). In Section 3, the convergence properties of the nonlinear estimator are proved. Then, the global estimation strategy and the method to tune the filter parameters are presented in Section 4. Finally, the proposed vehicle localization system is validated through simulation (in Section 5) and experimental results (in Section 6) in urban area: the convergence properties of the estimator and its robustness to low speed and GPS loss are especially highlighted.

## 2. Physical system

### 2.1. Motion equations

The Earth is considered flat and defining an inertial frame. The vehicle is supposed to move in a plane. It also assumed that the vehicle velocity vector is always tangent to the trajectory (as in [Bonnabel et al., 2008](#); [Dissanayake et al., 2001](#); [Fiengo et al., 2009](#)). In this case, the motion of the vehicle is described by the following nonholonomic equations:

$$\dot{\psi} = \omega,$$

$$\dot{p}^n = \|v\| \cos \psi,$$

$$\dot{p}^e = \|v\| \sin \psi,$$

where  $\psi$  is the yaw angle (or heading);  $\omega$  is the instantaneous angular velocity vector around vertical;  $p = (p^n, p^e)$  and  $v = (v^n, v^e) = (\dot{p}^n, \dot{p}^e)$  are the position and the velocity vectors of the center of mass with respect to the Earth-fixed frame in North-East coordinates.

### 2.2. Measurements

Three kinds of sensors are used: one low-cost gyroscope measures  $\omega_m = \omega + \omega_b$ , where  $\omega_b$  is a constant vector bias; two wheel speed sensors “measure” the speed of the left and the right wheel (more rigorously, these sensors measure the angular velocity, which is multiplied afterwards by the radius of the wheel to get the speed), resp.  $u^l$  and  $u^r$ , such that these sensors are

seen as one single speedometer that measures the scalar quantity  $v_s = (u^l + u^r)/2s = (1/s)\|v\|$ , where  $s > 0$  is a constant scaling corresponding to the uncertainty on the wheel radius (it is practically relevant to assume  $s \sim 1$ ); the position and velocity vectors  $p$  and  $v$  are provided by the navigation solutions  $y_p = (y_{p^n}, y_{p^e}) = (p^n, p^e)$  and  $y_v = (y_{v^n}, y_{v^e}) = (v^n, v^e)$  of a GPS engine. Notice that the wheel speed can be easily measured from the signals of the anti-lock braking system (ABS)-dedicated sensors via the analog to digital converter bus. These sensors provide accurate measurements of the wheel angular velocity. If no such wheel speed measurements is available, the estimation strategy proposed in this paper can still be used replacing  $sv_s$  with the norm of the GPS velocity  $(y_{v^n}^2 + y_{v^e}^2)^{1/2}$ . The resulting observer was experimentally tested in urban areas (with GPS available), and leads to results similar to those presented in Sections 5 and 6.

The vector bias  $\omega_b$  is a well-known low-cost gyroscope imperfection model. Its value can be first estimated when the vehicle is at rest, but it needs to be re-estimated (or reset) when the vehicle is moving, since this “slowly time-varying” bias may depend on external parameters such as temperature. The variations of the bias over the time is the major drawback of low-cost gyroscope. Similarly, the scaling  $s$  on the velocity measurement  $v_s$  provided by the speedometer models some uncertainty in the diameter of the wheels. This scaling is also “slowly time-varying” as it depends on changing parameters such as pressure in the wheel and tire wear. Notice that the scaling  $s$  cannot be estimated when the vehicle is at rest. Nevertheless, a “constant” model for these two imperfections is considered: this assumption is standard for online parameter estimation, as  $\omega_b$  and  $s$  are continuously estimated by the proposed filter when the vehicle moves and the GPS is available. The GPS is assumed to be relatively inaccurate, so that only its average effect is used over several seconds, which is standard in usual GPS-aided inertial navigation methods. Contrary to the GPS, the gyroscope and speedometer measurements are supposed to be always available as their availability does not depend on the environment features. Noise also corrupts all the measurements: it is not explicitly written in the model (contrary to Kalman method—based on filters). Indeed, evaluating the noise is not a simple task, and assuming that the GPS and other sensors’ noise is Gaussian is anyway questionable. The noise is indirectly taken into account in the tuning of the estimator gains (as for any Luenberger-type observer).

### 2.3. Considered model

From the preceding sections, the system considered to design the observer is

$$\dot{\psi} = \omega_m - \omega_b, \quad (1)$$

$$\dot{p}^n = sv_s \cos\psi, \quad (2)$$

$$\dot{p}^e = sv_s \sin\psi, \quad (3)$$

$$\dot{\omega}_b = 0, \quad (4)$$

$$\dot{s} = 0, \quad (5)$$

with the output (when GPS measurements are available)

$$\begin{pmatrix} y_{p^n} \\ y_{p^e} \\ y_{v^n} \\ y_{v^e} \end{pmatrix} = \begin{pmatrix} p^n \\ p^e \\ v^n \\ v^e \end{pmatrix} = \begin{pmatrix} p^n \\ p^e \\ sv_s \cos\psi \\ sv_s \sin\psi \end{pmatrix} \quad (6)$$

and known input (from gyroscope and speedometer measurements, which are assumed always available)

$$\begin{pmatrix} u_\omega \\ u_s \end{pmatrix} = \begin{pmatrix} \omega_m \\ v_s \end{pmatrix}. \quad (7)$$

When GPS measurements are available and the vehicle is moving ( $v_s \neq 0$ ), the system (1)–(7) is observable since all the state variables can be recovered from the known quantities  $\omega_m$ ,  $v_s$ ,  $y_{p^n}$ ,  $y_{p^e}$ ,  $y_{v^n}$ ,  $y_{v^e}$ , and their derivatives: from (6) one gets  $p^n = y_{p^n}$ ,  $p^e = y_{p^e}$ ,  $s = \sqrt{(y_{v^n}^2 + y_{v^e}^2)}/v_s^2$ , and  $\psi = \arctan(y_{v^e}/y_{v^n})$  if  $y_{v^n} \neq 0$ ,  $\psi = \text{sign}(y_{v^e})(\pi/2)$  otherwise. Finally, (1) yields  $\omega_b = \omega_m - \dot{\psi}$ . Therefore, it is possible to construct a filter to estimate the state variables from measurements (6), (7). When GPS measurements are not available, the output (6) cannot be used anymore to estimate the state variables. Since the system (1)–(5) becomes unobservable, the estimator boils down to a copy of the initial system (1)–(5), without any correction terms (open-loop).

## 3. Nonlinear observer equations and convergence properties

### 3.1. Nonlinear observer equations

The goal of this section is to present the nonlinear observer used for the system (1)–(7), when the GPS signal is available and used in the filtering algorithm. The observer is based on the symmetry-preserving observers’ theory recently introduced and developed in Bonnabel et al. (2008). The idea of such observers is to design nonlinear estimators whose structure mimics the nonlinearities of the trusted dynamic model. The resulting observers possess the same natural symmetries and invariance properties as the considered system. Such candidate symmetry-preserving observers can be determined from the constructive method described in Bonnabel et al. (2008). These observers possess very nice features from an engineering viewpoint (e.g. tuning and implementation simplicity) and strong properties for a theoretical matter (e.g. convergence around a large set of trajectories). Such symmetry-preserving observers have already been successfully designed and implemented for generic AHRS (in Martin & Salaün 2007, 2010) and aided AHRS (see Martin & Salaün 2008a, 2008b). Some other recent works have independently advocated the use of such observers as valuable alternatives to Kalman filtering for attitude estimation and localization systems (see e.g. Hamel & Mahony, 2006; Mahony, Hamel, & Pfimlin, 2008 for AHRS and Lageman et al., 2010; Vasconcelos, Cunha, Silvestre, & Oliveira, 2007; Vasconcelos et al., 2008 for aided AHRS). Built on preliminary results in Guillaume and Rouchon (1998) and Bonnabel et al. (2008), a symmetry-preserving nonlinear observer is proposed, as a valuable algorithm for vehicle localization system.

The equations of the nonlinear observer are the following:

$$\frac{d}{dt} \hat{\psi} = \omega_m - \hat{\omega}_b + k_\psi (\cos(\hat{\psi})y_{v^e} - \sin(\hat{\psi})y_{v^n}), \quad (8)$$

$$\frac{d}{dt} \hat{p}^n = \hat{s}v_s \cos\hat{\psi} + k_p (y_{p^n} - \hat{p}^n), \quad (9)$$

$$\frac{d}{dt} \hat{p}^e = \hat{s}v_s \sin\hat{\psi} + k_p (y_{p^e} - \hat{p}^e), \quad (10)$$

$$\frac{d}{dt} \hat{\omega}_b = -k_b \hat{s}v_s (\cos(\hat{\psi})y_{v^e} - \sin(\hat{\psi})y_{v^n}), \quad (11)$$

$$\frac{d}{dt} \hat{s} = k_s \hat{s} (\max(\cos(\hat{\psi})y_{v^n} + \sin(\hat{\psi})y_{v^e}, v_s \epsilon) - \hat{s}v_s), \quad (12)$$

with  $k_\psi, k_p, k_b, k_s > 0$ , and  $\epsilon > 0$  is small enough (in the sequel, it is assumed  $s/2 > \epsilon > 0$ ). Indeed, as  $s$  is close to 1 in the simulation,

it is typically chosen  $\epsilon = 1/5$ ). The velocity estimation, which implicitly appears in (9), (10), is directly given by

$$\hat{v}^n = \hat{s}v_s \cos \hat{\psi},$$

$$\hat{v}^e = \hat{s}v_s \sin \hat{\psi}.$$

Some nice features of the proposed observer (8)–(12) are obvious:

- Easy to implement and computationally thrifty: only few multiplications and additions between scalars are necessary to run the filtering algorithm.
- Easy to tune: only four gains to choose, and the tuning method is natural and easy thanks to a cascade structure of the filter equations (to be detailed in Section 4).
- Invariance to any non-trivial choice of coordinates: the estimation quality is independent of the direction of the Earth-fixed frame. Indeed, if one writes the observer equations in a frame whose first axis is pointing towards South–West instead of East, the observer equations will look exactly the same (see Section 4 and more generally Bonnabel et al., 2008 for more details).
- $\hat{s}(t) > 0$  provided  $\hat{s}(0) > 0$ : the (physical) constraint on the sign of the scaling  $s$  is automatically respected (as proved by Lemma 2).
- No problem at low speed: there is no division between measurements having a possibly degraded signal-to-noise ratio (especially, the term  $\arctan(y_{ve}/y_{vn})$  is never computed), and no division by the (possibly very small) term  $v_s$  is involved.

In order to illustrate the type of problems that can occur with divisions at low speed, let us consider one example. Suppose for instance that  $w$  is a white additive Gaussian noise corrupting  $y_{vn}$ . When  $y_{vn}$  is close to zero,  $y_{ve}/y_{vn}$  can be approximated by  $y_{ve}/w$ , and  $\arctan(y_{ve}/y_{vn})$  can then arbitrarily be close to  $\pi/2$  and also to  $-\pi/2$  several times over a very short period.

### 3.2. Error system

Beyond the preceding features, a major advantage of the proposed observer (8)–(12) is its large domain of convergence. From practical viewpoint, “large domain of convergence” means that the convergence of the estimator can be guaranteed around a large set of usual trajectories followed by a vehicle. The convergence of the observer will be analyzed thanks to the state error

$$\begin{pmatrix} \tilde{\psi} \\ \tilde{p}^n \\ \tilde{p}^e \\ \tilde{\omega}_b \\ \tilde{s} \end{pmatrix} = \begin{pmatrix} \hat{\psi} - \psi \\ \hat{p}^n - p^n \\ \hat{p}^e - p^e \\ \hat{\omega}_b - \omega_b \\ \hat{s} - s \end{pmatrix}.$$

The main benefit of such a nonlinear observer is that the (non-linear) state error equation has the following nice structure:

$$\frac{d}{dt} \tilde{\psi} = -\tilde{\omega}_b - k_\psi s v_s \sin(\tilde{\psi}), \quad (13)$$

$$\frac{d}{dt} \tilde{p}^n = (\hat{s}v_s \cos \hat{\psi} - s v_s \cos \psi) - k_p (\tilde{p}^n), \quad (14)$$

$$\frac{d}{dt} \tilde{p}^e = (\hat{s}v_s \sin \hat{\psi} - s v_s \sin \psi) - k_p (\tilde{p}^e), \quad (15)$$

$$\frac{d}{dt} \tilde{\omega}_b = k_b \hat{s} s v_s^2 \sin(\tilde{\psi}), \quad (16)$$

$$\frac{d}{dt} \tilde{s} = k_s \hat{s} v_s (\max(\cos(\tilde{\psi}), \epsilon) - \hat{s}). \quad (17)$$

The error system breaks into two subsystems: (13), (16), (17) and (14), (15). Convergence of the subsystem (14), (15) is

straightforward as soon as (13), (16), (17) has converged. The article will thus focus on this second system. A very nice property of this subsystem is that it is independent of the vehicle trajectory  $(\psi(t), \omega(t))$ . Indeed, although the system is non-linear, the error only depends on the errors  $\tilde{\psi}$ ,  $\tilde{\omega}$ , and on  $\hat{s}, v_s$  (instead of  $\tilde{\psi}, \psi, \tilde{\omega}, \omega$ , and  $\hat{s}, s, v_s$ ). This property plays a key role in the strong convergence properties of the observer.

### 3.3. Convergence properties of the observer

In the following sections, the different convergence properties are detailed. From a mathematical standpoint, the difficulties stem from the fact that the considered system is nonlinear, time-varying, and divisions by possibly small (noisy) terms such as  $v_s, y_{vn}, y_{ve}$  must be avoided. As a reminder, it is important to notice that the initial system (1)–(5) is observable only if  $v_s \neq 0$ . Therefore, an underlying condition to get convergence properties of the proposed estimator is that  $v_s \neq 0$ , i.e. the vehicle moves. If the vehicle stops, i.e.  $v_s = 0$  (or in practice under a very small threshold, whose value is a function of the sensor accuracy), the equations of the nonlinear observer (8)–(12) become

$$\frac{d}{dt} \hat{\psi} = \omega_m - \hat{\omega}_b,$$

$$\frac{d}{dt} \hat{p}^n = k_p (y_{pn} - \hat{p}^n),$$

$$\frac{d}{dt} \hat{p}^e = k_p (y_{pe} - \hat{p}^e),$$

$$\frac{d}{dt} \hat{\omega}_b = 0,$$

$$\frac{d}{dt} \hat{s} = 0.$$

Contrary to the estimated position that is still corrected using the GPS position measurements, the estimated bias and scaling are not updated anymore, and the yaw angle is estimated in open-loop. This behavior advocates the use of a filter with guaranteed properties to perpetually estimate the gyroscope bias and speedometer scaling, when the vehicle moves and the GPS signal is available. Then in the sequel, it is assumed that the vehicle never stops, i.e.  $v_s \neq 0$ .

#### 3.3.1. Local convergence around a very large set of trajectories

The following theorem proves that the proposed observer converges around *any trajectory* followed by the system, under some assumptions on the vehicle speed that are practically relevant.

**Theorem 1.** Consider the system (1)–(5). Assume there exists three scalars  $M_1, M_2, \bar{M}_2 > 0$  such that the speed  $v_s$  satisfies

$$\frac{d}{dt} v_s < M_1 v_s^2, \quad M_2 \leq v_s^2 \leq \bar{M}_2. \quad (18)$$

Take  $k_p, k_b > 0$  and  $k_\psi > M_1/s$ . The nonlinear observer (8)–(12) converges around any trajectory of the time-varying system.

The proof is given in Appendix A. The assumptions above are not restrictive and apply to normal driving conditions.

#### 3.3.2. Almost global convergence in case of constant velocity

The following theorem ensures that the observer converges almost globally when the norm of the vehicle speed is constant, which is approximately the case most of the time under normal driving conditions.

**Theorem 2.** Consider the system (1)–(5). Assume the speed  $v_s$  is constant over the time. Set  $k_\psi, k_b, k_p > 0$ , and  $\hat{s}(0) > \epsilon$ . Let  $A = \max(\hat{s}(0), s)$ . For  $0 < k_s \leq k_\psi s / (4A)$ , the nonlinear observer (8)–(12) is such that

- the error  $(\tilde{\psi}, \tilde{p}^n, \tilde{p}^e, \tilde{\omega}_b, \tilde{s})$  is locally exponentially stable to 0;
- for almost any initial conditions, the error asymptotically converges to 0.

“Almost any” means that the set of initial conditions such that the error does not converge to zero is of null measure in the overall space. Thus, if the observer is initialized inside this set a small perturbation (such as gyroscope measurement noise) will make it move out of the set. So global convergence is always expected in practice.

3.3.3. Global convergence with a known bias

It is usually argued in the literature that the gyroscope bias  $\omega_b$  is very slowly time-varying, and then can be estimated for good when the vehicle is at rest. As previously mentioned, in practice the lack of stability in time of the biases is the major drawback of low-cost gyroscopes. Indeed, whereas a large gyro white noise is easily handled using any Luenberger observer or Kalman filter, an inefficient bias estimation leads to degraded performance of the localization system. From a theoretical viewpoint, assuming a known constant bias simplifies drastically the convergence analysis. In this case, the proposed observer ensures exponential convergence of the nonlinear time-varying system for any initial condition except  $\hat{\psi}(0) = \pi$ . Indeed, one gets the following formal result:

**Theorem 3.** Consider the system (1)–(5). Assume  $\int_{t_0}^\infty |v_s(t)| dt = \infty$  for all  $t_0 > 0$ . The nonlinear observer (8)–(10), (12) with  $k_\psi, k_p, k_s > 0$ ,  $\hat{s}(0) \geq \epsilon$ , and  $\hat{\omega}_b \equiv \omega_b$ , is such that the error globally converges to 0 for any initial condition, except  $\hat{\psi}(0) = \psi(0) + \pi + 2k\pi$  with  $k \in \mathbb{Z}$ . Moreover, the convergence is exponential in the time scale  $dt = v_s dt$ .

The proof is given in Appendix C. The assumption  $\int_{t_0}^\infty |v_s(t)| dt = \infty$  for all  $t_0 > 0$  is not restrictive and it is standard for these kind of systems, since the system is unobservable if  $v_s = 0$ . In particular, it is satisfied in case of lower bounded velocity  $v_s$ .

4. Estimation strategy and gains tuning

The global estimation strategy is shown in Fig. 1. When GPS is available, the nonlinear observer (8)–(12) is used to provide estimations. If GPS is not available, an open-loop estimator gives the estimated state of the vehicle. In this section, an easy way to tune the different gains of the nonlinear observer is proposed, and the equations of the open-loop estimator are given. With the recommended tuning proposed in this section (minimizing the integral of time and absolute error—ITAE—criterion; see Nagrath

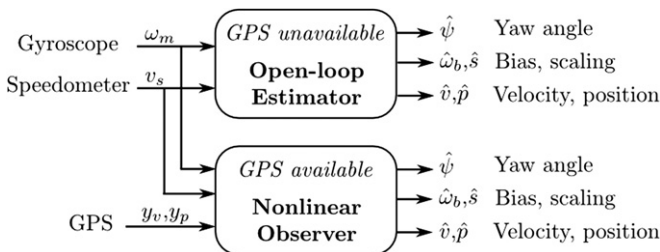


Fig. 1. Global architecture of the proposed estimation strategy.

& Gopal, 2006 for details on this performance criterion), only two gains are left to the user. A very simple tuning strategy of those two remaining gains is based on the signal-to-noise ratio of the system under consideration.

Since it is not the main contribution of this paper, details on implementation of the proposed strategy and algorithms, such as signal processing, transition with/without GPS, or checking reliability of GPS to adjust the filter gains (e.g. taking into account the dilution of precision value), are not given.

4.1. Nonlinear observer when GPS is available

The nonlinear observer (8)–(12) can be decomposed into three in cascade subfilters,  $F_g, F_s, F_{vp}$ , as illustrated in Fig. 2:

- Filter  $F_g$  provides estimated yaw angle and gyro bias,  $\hat{\psi}, \hat{\omega}_b$ . It has two gains to choose,  $k_\psi, k_b$ .
- Filter  $F_s$  estimates the scaling of the speedometer,  $\hat{s}$ . It has one gain to choose,  $k_s$ .
- Filter  $F_{vp}$  finally gives the estimation of the vehicle velocity and position,  $\hat{v}, \hat{p}$ . It has one gain to choose,  $k_p$ .

This natural structure allows an easy tuning of the different parameters of each filter, as detailed below. In fact, with the tuning recommended below (minimizing the ITAE performance criterion, and consistent with the theorems above), only two gains are left to the user: a first one to tune the convergence rate of the velocity filter, and another one to tune the convergence rate of the position filter.

4.1.1. Filter  $F_g$

The equations of filter  $F_g$  are

$$\frac{d}{dt} \hat{\psi} = \omega_m - \hat{\omega}_b + k_\psi (\cos(\hat{\psi}) y_{v^e} - \sin(\hat{\psi}) y_{v^n}), \tag{19}$$

$$\frac{d}{dt} \hat{\omega}_b = -k_b \hat{s} v_s (\cos(\hat{\psi}) y_{v^e} - \sin(\hat{\psi}) y_{v^n}), \tag{20}$$

with  $k_\psi, k_b > 0$ . Note that the observer possesses the same invariance properties (symmetries) as the standard system. Indeed (19), (20) are invariant to a change of origin of the angles  $\psi \mapsto \psi + \psi_0$  and  $\hat{\psi} \mapsto \hat{\psi} + \psi_0$ , as  $\cos(\hat{\psi}) y_{v^e} - \sin(\hat{\psi}) y_{v^n} = -s v_s \sin(\hat{\psi} - \psi)$  and then  $\hat{\psi} - \psi = (\hat{\psi} + \psi_0) - (\psi + \psi_0)$ . It is easy to check the same invariance by rotation of the initial system (1)–(5).

The gains can be tuned thanks to the following nice feature:

**Lemma 1.** Assume  $\hat{s} = s$ , and  $v_s$  is fixed. Let  $k_\psi = 2\gamma\zeta$  and  $k_b = \gamma^2$ . Then the linearized equation around  $\tilde{\psi} = 0$  becomes

$$\frac{d^2}{dt^2} \tilde{\psi} + 2\zeta\omega_0 \frac{d}{dt} \tilde{\psi} + \omega_0^2 \tilde{\psi} = 0,$$

where  $\omega_0 = \gamma s v_s$ .

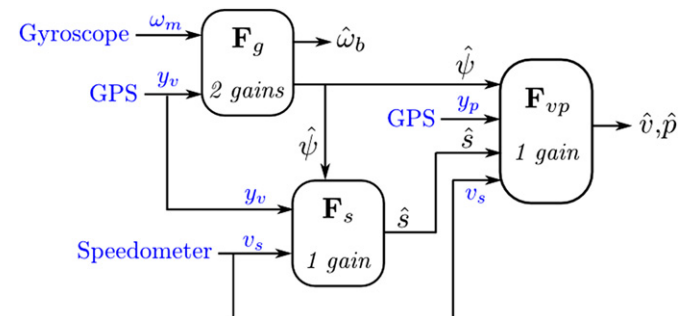


Fig. 2. Interaction between the three subfilters of the nonlinear observer.

The linearized error equation around  $\tilde{\psi} = 0$  is the motion of a damped linear oscillator, whose frequency is proportional to the car speed  $v_s$ . The observer is thus very natural as it provides a tuning of the gains which automatically adapts to the speed of the car: the convergence rate is proportional to the velocity (up to a  $\gamma$  factor chosen by the user). The faster the car goes, the easier the state is to identify, the faster the observer converges. In fact, such a tuning yields a convergence rate which is proportional to signal-to-noise ratio (SNR) of the GPS velocity output (admitting the noise is additive). So  $\gamma$  must be tuned according to the SNR of the GPS velocity signal.

In practice it is recommended to take  $\xi = \frac{\sqrt{\gamma}}{2}$ , minimizing the ITAE performance criterion. So there is in fact only one gain  $\gamma$  to choose.

4.1.2. Filter  $F_s$

The equation of filter  $F_s$  is

$$\frac{d}{dt} \hat{s} = k_s \hat{s} (\max(\cos(\hat{\psi})y_{vm} + \sin(\hat{\psi})y_{ve}, v_s \epsilon) - \hat{s}v_s), \tag{21}$$

with  $0 < k_s \leq k_\psi s / (4A)$ . As  $s$  is approximately known, it is sensible to assume  $A = \max(\hat{s}(0), s) \leq 1.5s$ , and thus one must take  $k_s \leq k_\psi / 6$ . As  $k_\psi = 2\gamma\xi$  a very good choice in practice is

$$k_s = 0.1\gamma = \sqrt{k_b} / 10$$

provided the filter  $F_g$  is tuned as suggested. Note that  $\hat{s}$  is generally well initialized, as the wheel radius is approximately known.

4.1.3. Filter  $F_{vp}$

The equations of filter  $F_{vp}$  are

$$\hat{v} = \hat{s}v_s(\cos(\hat{\psi}), \sin(\hat{\psi})), \tag{22}$$

$$\dot{\hat{p}} = \hat{v} + k_p(y_p - \hat{p}), \tag{23}$$

with  $k_p > 0$ . Eq. (22) directly gives the velocity estimation as a function of  $\hat{\psi}, \hat{s}$  and  $v_s$ . The gain  $k_p$  represents the coefficient used to correct the GPS position estimations with the (accurate) velocity estimation. As the GPS update rate is usually low (1–4 Hz),  $F_{vp}$  allows moreover to estimate the evolution of  $p$  at higher refreshment rate (typically 50–100 Hz).

4.2. Open-loop estimator when GPS is unavailable

If GPS is unavailable (or too inaccurate to be truly used), an open-loop estimator is used, whose equations are a copy of the dynamics of the considered system (1)–(5), i.e.

$$\dot{\hat{\psi}} = \omega_m - \hat{\omega}_b, \tag{24}$$

$$\dot{\hat{\omega}}_b = 0, \tag{25}$$

$$\dot{\hat{s}} = 0, \tag{26}$$

$$\hat{v} = \hat{s}v_s(\cos(\hat{\psi}), \sin(\hat{\psi})), \tag{27}$$

$$\dot{\hat{p}} = \hat{v}. \tag{28}$$

Such an open-loop observer heavily relies on the validity of the initial estimates (at the time where the GPS signal is lost), advocating the use of a filter with guaranteed properties to perpetually estimate the gyro bias and speedometer scaling, when GPS is available.

The transition from the mode “GPS available” to the mode “GPS unavailable” (and vice-versa) is naturally done, because the same structure of Eqs. (8)–(12) are in fact used for the two modes; only the correction terms change. In other terms, the initial conditions of the “new” filter are the last estimates of the

previous observer. This simple choice leads to a smooth estimated trajectory, without any jump when switching between the two modes. Other switching strategies may be considered, e.g. initializing the new variables close to the GPS measurements when it becomes available, if the estimated position given by the open-loop estimator (24)–(28) are very far from the first recovered GPS measurements. Nevertheless, for simplicity, only the “natural” switching strategy is considered in this paper. Its nice behavior can be seen through the simulation and experiment results given in Sections 5 and 6.

5. Simulation results

The proposed estimation strategy and algorithms are first validated through simulation. To simulate a realistic setup, noise is added on the measurements, which leads to consider the following system:

$$\dot{\psi} = \omega_m - \omega_b + w_\psi,$$

Table 1  
Noise variances (simulation).

Noise	Variance (SI)
$w_\psi$	1e–2
$w_p$	1e–2
$w_\omega$	3e–4
$w_s$	1e–2
$w_{y_p^e}, w_{y_p^m}$	1.5
$w_{y_p^e}, w_{y_p^m}$	1e–2

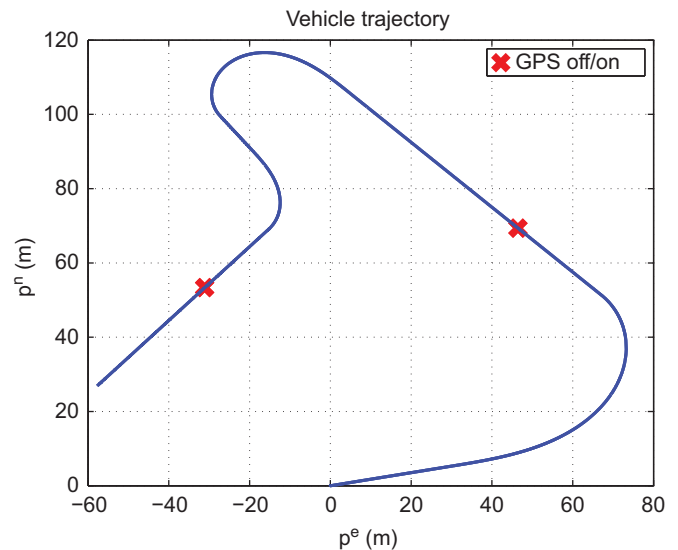


Fig. 3. True vehicle trajectory (simulation).

Table 2  
Initialization errors (simulation).

Estimated state	Case 1—C1	Case 2—C2
Yaw angle	90°	180°
Velocity	2 m/s	3 m/s
Position	3 m	2 m
Gyro bias	0.1°/s	0.15°/s
Scaling	0.1	0.15

$$\dot{p}^n = s(v_s + w_p)\cos\psi,$$

$$\dot{p}^e = s(v_s + w_p)\sin\psi,$$

$$\dot{\omega}_b = w_\omega,$$

$$\dot{s} = w_s,$$

with the output (when GPS measurements are available)

$$\begin{pmatrix} y_{p^n} \\ y_{p^e} \\ y_{v^n} \\ y_{v^e} \end{pmatrix} = \begin{pmatrix} p^n + W_{y_{p^n}} \\ p^e + W_{y_{p^e}} \\ v^n + W_{y_{v^n}} \\ v^e + W_{y_{v^e}} \end{pmatrix}.$$

The noises  $w_i$  are independent normally distributed random scalar with mean 0 and variance defined by Table 1 (notice it is

the value of the variance noise in SI and not the value of the standard deviation that is mentioned in Table 1). As illustrated in Fig. 4(b), measurements provided by the gyroscope are very noisy. Indeed, the signal-to-noise ratio for the gyroscope measurement is only 16 dB. The wheel diameter value also evolves quite quickly (see Fig. 4(c)), in order to consider an unfavorable scenario. The true vehicle trajectory is shown in Fig. 3, where the coordinates of the starting point are (0,0). Equations of nonlinear observer (when GPS is available) and open-loop estimator (when GPS is unavailable) are given in Section 4. The gains of the estimator are set to  $k_\psi = 0.21$ ,  $k_b = 2.3e-2$ ,  $k_s = 1.5e-2$ ,  $k_p = 0.7$  and  $\epsilon = 0.2$ .

To illustrate the large domain of convergence of the proposed filtering algorithm, the estimator is badly initialized, that is the estimated state is initialized far from its true value, as summarized in Table 2 (the initialization errors in velocity and in position

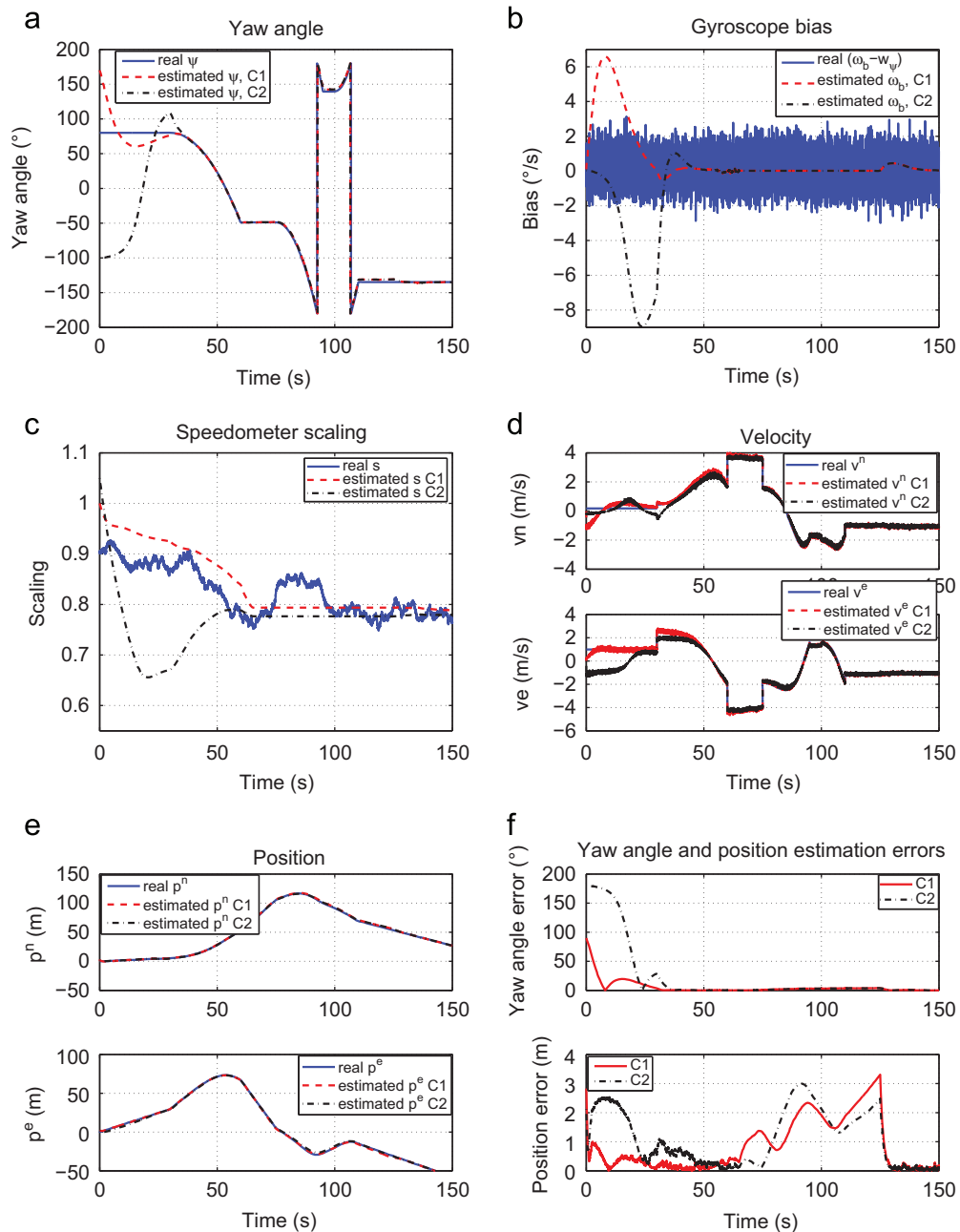


Fig. 4. Global behavior with bad initialization and GPS unavailable between 65 and 125 s (simulation). (a) Yaw angle. (b) Gyroscope bias. (c) Speedometer scaling. (d) Vehicle velocity. (e) Vehicle position. (f) Yaw angle and position estimation absolute errors.

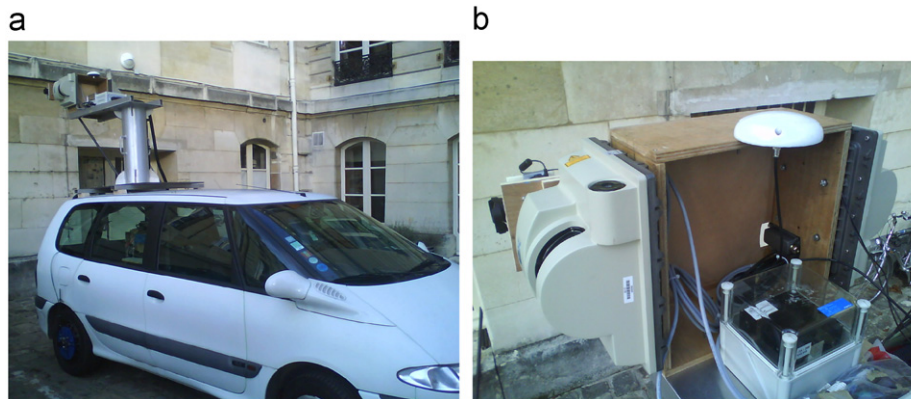


Fig. 5. Experimental setup. (a) Vehicle used for tests. (b) GPS and gyroscope on the roof.

are especially exaggerated to illustrate the large domain of convergence of the estimator). Fig. 4 shows that the observers converge despite very wrong initial values. Notice that the yaw angle is well estimated, even if the speed of the vehicle is very low. Between 65 and 125 s, a loss of GPS is simulated. Estimations remain “good” when GPS becomes unavailable (errors in yaw angle estimation of less than  $4^\circ$ , and errors in position of less than 3.5 m), even with very noisy gyro measurements. As soon as GPS signal can be used again in the correction terms (at  $t=125$  s), the estimations converge well to the right values.

## 6. Experimental validation

### 6.1. Experimental setup

The proposed vehicle localization system is now validated through experiment results. Two pictures of the experimental setup are shown in Fig. 5, with the vehicle used (a Renault Espace, see Fig. 5(a)) and the gyroscope and GPS antenna installed on the roof (see Fig. 5(b)). The trajectory followed by the vehicle is a turn around the “Place du Châtelet”, at the center of Paris (France), in order to illustrate the good behavior of the filter in urban areas, where GPS measurements are likely to be inaccurate or even unavailable. The vehicle moves at very low speed (around 10 km/h).<sup>1</sup>

Measurements from z-axis Crossbow VG600 gyroscope (update rate 84 Hz) and GPS Trimble AG132 antenna (update are 10 Hz) are used. In addition, two wheel speed sensors provide measurements at 10 Hz. The two speed wheel sensors can be found in most of the cars (coming from ABS), and measure the number of turn per second,  $n^l$  and  $n^r$  for the left and the right wheel. From  $n^l$  and  $n^r$ , the left and right wheel speeds are directly computed:  $u^l = a(2\pi)n^l$  and  $u^r = a(2\pi)n^r$ , where  $a$  is the radius of the wheel. The vehicle characteristics give  $a=31.725$  cm. Any error and unbalance in the value of  $a$  is compensated by considering the scaling  $s$  in the filter equations. A computer gathers all information and gives estimations in real-time at 84 Hz, using a simple Euler explicit approximation for

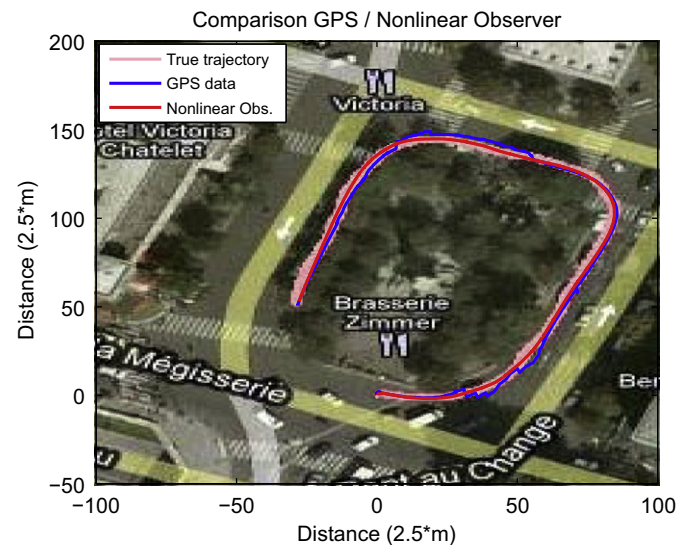


Fig. 6. Global behavior of the nonlinear observer (experiment).

the integration scheme. Equations of nonlinear observer (when GPS is available) and open-loop estimator (when GPS is unavailable) are given in Section 4, and the estimator gains are set to  $k_\psi = 0.21$ ,  $k_b = 2.3e-2$ ,  $k_s = 1.5e-2$ , and  $k_p = 0.15$ . The gain  $k_p$  is smaller than in Section 5 because the GPS measurements are here more inaccurate (long periods of “jump” of GPS position measurement, as it can be seen in Fig. 6).

### 6.2. Global behavior

First, the good behavior of the proposed nonlinear filter is illustrated, when GPS is available. The vehicle is at rest during 20 s to check data transmission, and then turns around the “Place du Châtelet”. The filter estimations are well initialized. Especially, the gyroscope bias is estimated at rest (averaging the gyroscope measurements), as well as the yaw angle, thanks to the known starting direction of the vehicle. As seen in Fig. 6, the estimated trajectory of the vehicle is very close to the true trajectory, despite a low speed of the vehicle, and inaccurate GPS measurements due to the surrounding buildings and trees.

### 6.3. Bad initialization

The convergence properties of proposed estimator, when GPS is available, are now put in evidence. Therefore, the filtering

<sup>1</sup> The vehicle used to run the experiments is dedicated to mapping of urban environment, using an embedded laser range finder (see Fig. 5(b)). Indeed, mobile mapping systems (MMS) acquire road and surrounding features information via several sensors (telemeters, photocameras, videocameras), see e.g. Abuhadrous, Ammoun, Nashashibi, Goulette, and Laurgeau (2004) and Barber, Mills, and Smith-Voysey (2008). The acquired data are then used to build 3D maps of the road, buildings, etc. Those vehicles move at very low speed, because of the acquisition time, and the validity of the produced maps relies drastically on the performances of the VLS at very low speed (see Section 3). Accurate mapping of urban areas is a rapidly growing field, with example applications such as Google Streetview.

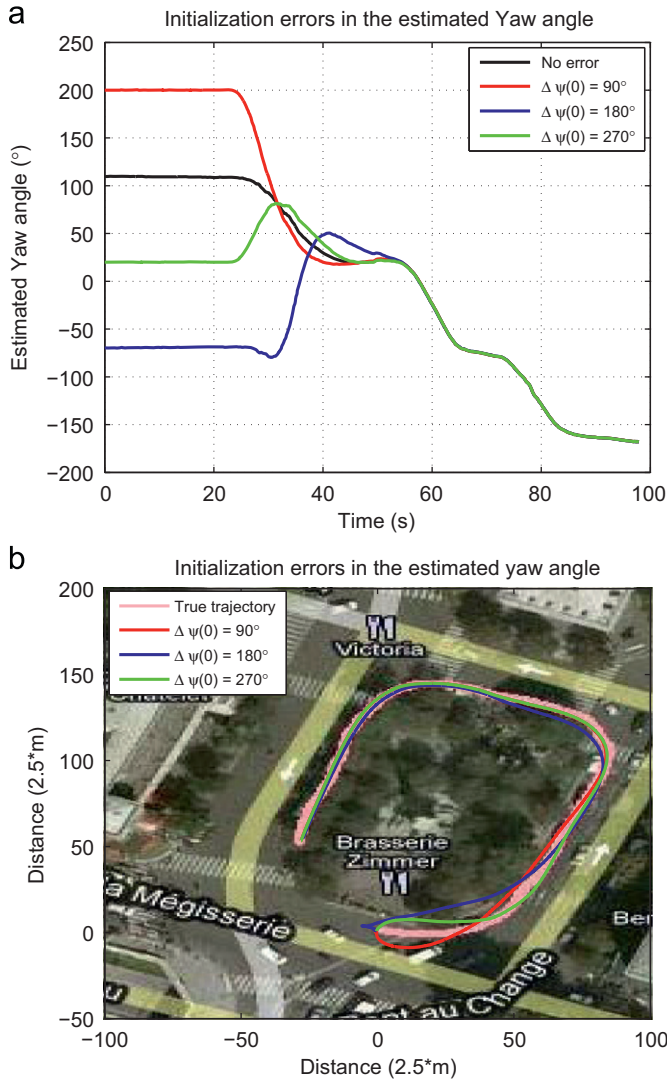


**Fig. 7.** Influence of initialization errors in the estimated yaw angle (experiment). (a) Evolution of estimated heading  $\hat{\psi}$ . (b) Estimated vehicle position.

algorithm is initialized with errors in the estimated yaw angle,  $\Delta\psi(0) = \hat{\psi}(0) - \psi(0)$ . Considering  $\Delta\psi(0) = 90^\circ, 180^\circ, 270^\circ$ , Fig. 7 illustrates the large domain of convergence of the proposed nonlinear estimator.

#### 6.4. Loss of GPS

The good performance of the estimation strategy when GPS becomes unavailable are finally highlighted. Considering the same raw data as in preceding experiment, GPS is artificially turned off between 34 and 78 s. Thanks to the nonholonomic constraints explicitly taken into account in the filtering algorithm, the estimated trajectory remains good when GPS is unavailable (see Fig. 8(a)) with a position error less than 2 m (see Fig. 8(b)). Furthermore, Fig. 8 illustrates the nice convergence of the nonlinear filter as soon as GPS is available again.

## 7. Conclusion

A low-cost localization system for ground vehicle has been proposed, using measurements from a few number of common sensors, i.e. one single-axis gyroscope, two wheel speed sensors and one GPS. Based on the nonholonomic constraints of the car,

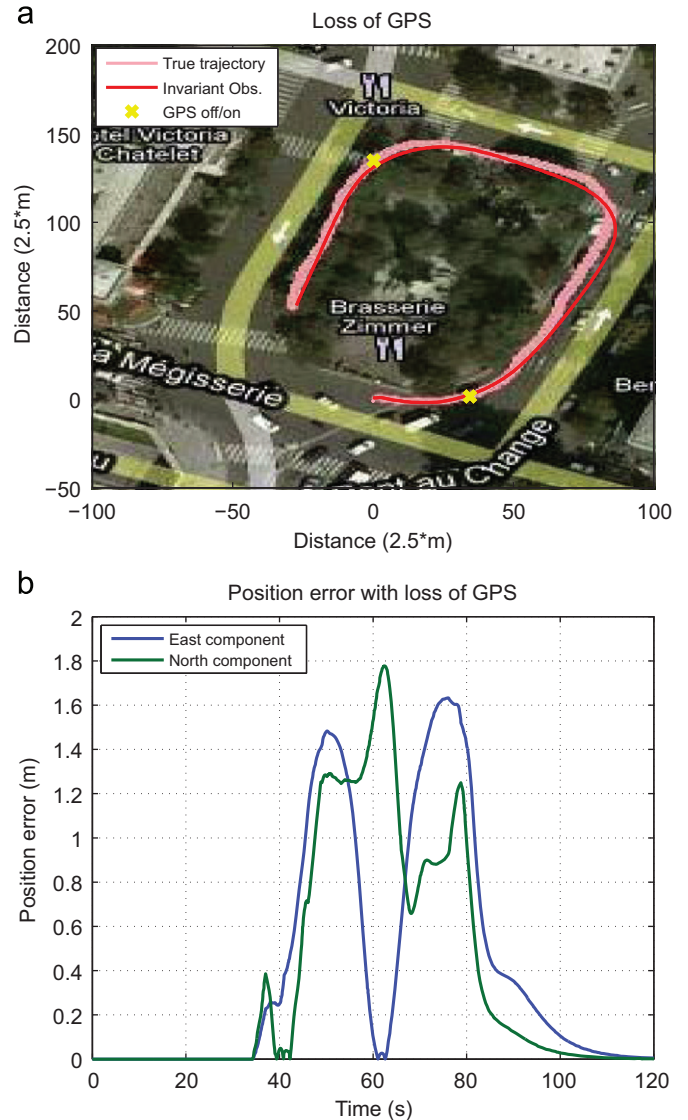


**Fig. 8.** GPS unavailable between 34 and 78 s (experiment). (a) Estimated vehicle position. (b) Evolution of the position absolute error.

the nonlinear estimator possesses very interesting features: it preserves natural symmetries of the system; it only has four parameters to tune, with a nice decoupled structure that allows an easy tuning; it is easy to implement and computationally thrifty; it continuously estimates the gyroscope bias and the uncertainty in the wheel diameter value; it keeps providing good estimations when GPS signal is very degraded or unavailable. Moreover, the proposed estimator has strong convergence properties that guarantee accurate estimations, even after a long GPS loss or a bad initialization.

It is believed that all the previously mentioned properties, highlighted and illustrated throughout the article, allow the proposed vehicle localization system to be a credible alternative to usual Kalman filter-based estimation strategies. It can be then considered as an adequate tool for generating accurate urban maps or for developing semi or fully automatic vehicles.

## Acknowledgments

The authors would like to thank Jean-Emmanuel Deschaud for running experiments and providing all data necessary for this

article. The authors also gratefully acknowledge Philippe Martin and Pierre Rouchon for their invaluable advices.

## Appendix A. Proof of Theorem 1

Proof of Theorem 1 in Section 3 is as follows.

**Proof.** This proof is inspired by Ignatyev (1997). The main goal is to prove convergence of the subsystem (13), (16), (17). When it has converged, the convergence of subsystem (14), (15) is obvious (indeed if  $\tilde{\psi}, \tilde{\omega}, \tilde{s}$  converge to zero, it implies that (14), (15) are linear equations in the variables  $\tilde{p}^n, \tilde{p}^e$  driven by bounded terms, and thus there is no peaking). The linearized subsystem (13), (16), (17) becomes

$$\frac{d}{dt}\tilde{\psi} = -\tilde{\omega}_b - k_\psi s v_s \tilde{\psi}, \quad (\text{A.1})$$

$$\frac{d}{dt}\tilde{\omega}_b = k_b (s v_s)^2 \tilde{\psi}, \quad (\text{A.2})$$

$$\frac{d}{dt}\tilde{s} = -k_s v_s \tilde{s}. \quad (\text{A.3})$$

Indeed, as  $\epsilon < s$ , the first-order approximation of  $\max(\cos(\tilde{\psi})s, \epsilon)$  around  $\tilde{\psi} = 0$  is  $s$ . The linearized system is made of two independent subsystems (A.1), (A.2) and (A.3). Subsystem (A.3) is linear, and it is straightforward that  $\tilde{s}$  tends exponentially to zero. Concerning subsystem (A.1), (A.2), consider the Lyapunov function

$$V = \frac{1}{2}(k_b (s v_s)^2 \tilde{\psi}^2 + \tilde{\omega}_b^2).$$

The derivative of  $V$  becomes

$$\frac{d}{dt}V = k_b s^2 v_s \left[ \frac{d}{dt}v_s - k_\psi s v_s^2 \right] \tilde{\psi}^2.$$

$\dot{V} \leq 0$  as  $(d/dt)v_s \leq M_1 v_s^2$  implies that  $(d/dt)v_s \leq k_\psi s v_s^2$ . As  $V$  is decreasing, it is bounded and  $(d/dt)V$  is integrable. As  $(d/dt)v_s - k_\psi s v_s^2 \leq (M_1 - k_\psi s) \underline{M}_2$ , which is a fixed negative scalar, it implies that  $\tilde{\psi}^2$  is integrable.  $\tilde{\psi}$  and  $\tilde{\omega}_b$  are bounded as  $V$  is bounded and  $v_s^2 > \underline{M}_2 > 0$ . Thus  $(d/dt)(\tilde{\psi})^2$  is bounded from (A.1), and applying Barbalat's lemma,  $(\tilde{\psi})^2 \rightarrow 0$  and thus  $\tilde{\psi} \rightarrow 0$ .

To prove  $\tilde{\omega} \rightarrow 0$ , let us prove that  $V \rightarrow 0$ . Indeed suppose that  $V(t)$  does not tend to zero. As  $V$  is monotonically decreasing, it means there exists  $\delta > 0$  such that for all  $t \geq 0$ ,  $V(t) \geq \delta$ . As  $(\tilde{\psi})^2 \rightarrow 0$  it implies there exists  $t_1 \geq 0$  such that for all  $t \geq t_1$  one has  $\tilde{\omega}_b^2(t) \geq \delta/2$ . As  $\tilde{\omega}_b$  is continuous, it implies that  $|\tilde{\omega}_b|$  is lower bounded by a strictly positive scalar. It yields a contradiction as it implies  $|\tilde{\psi}(t)|$  tends to infinity according to (A.1). Thus  $V(t)$  tends to 0 and  $\tilde{\omega}_b(t) \rightarrow 0$ .  $\square$

## Appendix B. Proof of Theorem 2

Proof of Theorem 2 in Section 3 is as follows.

**Proof.** The proof relies on the following preliminary result:

**Lemma 2.** Suppose  $\hat{s}(0) > \epsilon$ . Let  $A = \max(\hat{s}(0), s)$ . Then for any  $t \geq 0$   $\epsilon \leq \hat{s}(t) \leq A$ .

Let  $u(t) = \max(\cos(\tilde{\psi})s, \epsilon)$ . One has  $(d/dt)\hat{s} = k_s v_s \hat{s}(u(t) - \hat{s})$  with  $\epsilon \leq u(t) \leq A$ . Thus for arbitrary  $0 < \delta < \epsilon$ , the vector field is pointing inside the domain  $\mathcal{D}_\delta = \{x \in \mathbb{R} | x \geq \epsilon - \delta\}$ . Thus when  $\hat{s}(0) \in \mathcal{D}_\delta$ ,  $\hat{s}(t)$  cannot escape the domain  $\mathcal{D}_\delta$ . This is true for  $\delta$  arbitrarily small, which means that for all  $t \geq 0$ , one gets  $\hat{s}(t) \geq \epsilon$  (note it proves as a

by-product that  $\hat{s}(t) > 0$  provided  $\hat{s}(0) > 0$ ). A similar token allows to prove  $\hat{s}(t) \leq A$  for all  $t \geq 0$ .

Consider now the error subsystem (13), (16). Consider the candidate Lyapunov function

$$V = \hat{s}(1 - \cos(\tilde{\psi})) + \frac{1}{2k_b s v_s^2} \tilde{\omega}_b^2.$$

One has

$$\frac{d}{dt}V = \hat{s} v_s (-k_\psi s \sin(\tilde{\psi})^2 + k_s (u(t) - \hat{s})(1 - \cos(\tilde{\psi}))). \quad (\text{B.1})$$

There are two cases:

*Case1:*  $\cos(\tilde{\psi})s \leq \epsilon$ . Thus  $u(t) = \epsilon$ , and because of Lemma 2, one gets  $u(t) - \hat{s} \leq 0$ . It implies that  $(d/dt)V \leq -\epsilon v_s k_\psi s \sin(\tilde{\psi})^2 \leq 0$ , as for all  $t \geq 0$ ,  $\hat{s}(t) \geq \epsilon$ .

*Case2:*  $\cos(\tilde{\psi})s > \epsilon > 0$ . Then there exists  $k \in \mathbb{Z}$  such that  $|\tilde{\psi} - 2k\pi| < \pi/2$ . In the sequel, it is assumed without loss of generality that  $k \equiv 0$  (indeed one can always replace  $\tilde{\psi}$  in the following lines by  $\tilde{\psi} - 2k\pi$ ). Lemma 2 implies  $|u(t) - \hat{s}(t)| \leq 2A$ . Thus one obtains  $(d/dt)V \leq \hat{s} v_s (-k_\psi s \sin(\tilde{\psi})^2 + 4k_s A \sin(\tilde{\psi}/2)^2)$ . For  $k_s \leq k_\psi s / (4A)$  one gets  $(d/dt)V \leq -\hat{s} v_s k_\psi s (\sin(\tilde{\psi})^2 - \sin(\tilde{\psi}/2)^2)$ . For  $|\tilde{\psi}| \leq \pi/2$  one gets  $\sin(\tilde{\psi})^2 - \sin(\tilde{\psi}/2)^2 \geq \sin(\tilde{\psi})^2/2$ . Thus  $(d/dt)V \leq -\epsilon v_s k_\psi s \sin(\tilde{\psi})^2/2 \leq 0$ .

Thus  $(d/dt)V \leq 0$  for all  $t \geq 0$ . It implies that  $V$  is bounded. Thus  $\tilde{\omega}^2$  is bounded. Moreover as  $V(t) - V(0) = \int_0^t \dot{V}(s) ds$ ,  $\dot{V}$  is integrable. In both cases  $|\dot{V}| \geq \epsilon v_s k_\psi s \sin(\tilde{\psi})^2/2$ . It implies that  $\sin(\tilde{\psi}(t))^2$  is integrable. As  $(d/dt)\tilde{\psi}(t)$  is bounded, Barbalat's lemma proves that  $\sin(\tilde{\psi}(t))^2 \rightarrow 0$  when  $t \rightarrow \infty$  and thus  $\tilde{\psi} \rightarrow 0 + 2k\pi$  or  $\tilde{\psi} \rightarrow \pi + 2k\pi$  with  $k \in \mathbb{Z}$ . Moreover  $(d/dt)\tilde{\psi}$  is bounded. This implies using Barbalat's lemma again that  $(d/dt)\tilde{\psi} \rightarrow 0$  and thus  $\tilde{\omega} \rightarrow 0$ .

There are two cases. First, suppose that  $\tilde{\psi} \rightarrow 0 + 2k\pi$ . It implies that  $\hat{s} \rightarrow s$ . Indeed, as  $\hat{s}$  is bounded, there is no peaking. Thus  $\cos(\tilde{\psi})$  is replaced by 1 in (17), yielding the reduced system  $(d/dt)\tilde{s} = -k_s v_s \tilde{s} \hat{s}$ , proving convergence of  $\tilde{s}$  to 0. Studying the linearized system, one shows that  $(\tilde{\psi}, \tilde{\omega}, \tilde{s}) = (0 + 2k\pi, 0, s)$  is an exponentially stable equilibrium.

Then, suppose that  $\tilde{\psi} \rightarrow \pi + 2k\pi$ . By the same token as before, it implies  $\hat{s} \rightarrow \epsilon$ . Studying the linearized system, one shows that  $(\tilde{\psi}, \tilde{\omega}, \tilde{s}) = (\pi + 2k\pi, 0, \epsilon)$  is an unstable equilibrium, as the linear subsystem has one eigenvalue with strictly positive real part. There are trajectories that converge along the stable center manifold associated with the stable direction of the linearization around  $(\pi + 2k\pi, 0)$ . From the stable manifold theorem, the stable set of the equilibrium point is a manifold having the dimension of the stable set of the linearized system, i.e. it is of dimension 1. As a result, the set of trajectories that converge to this unstable equilibrium point is of null measure in overall space. This is why one writes  $\tilde{\psi} \rightarrow 0 + 2k\pi$  "almost" globally, as the probability of initializing the observer in the unstable set is null (for a random initialization).

Finally, exponential convergence of the error subsystem (14), (15) is straightforward for  $k_p > 0$  as soon as  $(\tilde{\psi}, \tilde{s})$  has converged to (0,0).  $\square$

## Appendix C. Proof of Theorem 3

Proof of Theorem 3 in Section 3 is as follows.

**Proof.** With  $\hat{\omega}_b = \omega_b$ , the error (13)–(17) becomes

$$\frac{d}{dt}\tilde{\psi} = -k_\psi s v_s \sin(\tilde{\psi}),$$

$$\frac{d}{dt}\tilde{s} = k_s \hat{v}_s (\max(\cos(\tilde{\psi}), s, \epsilon) - \tilde{s}).$$

Consider the regular change of time scale  $dl = v_s dt$ . Let us first focus on the first equation. One has  $d\tilde{\psi}/dl = -k_\psi \sin(\tilde{\psi})$ . The Lyapunov function  $V = 1 - \cos(\tilde{\psi})$  is such that  $dV/dl = -k_\psi \sin^2(\tilde{\psi}) \leq 0$ . Applying LaSalle's principle on the compact set  $\mathbb{S}^1$ ,  $\sin(\tilde{\psi})$  converges to zero when  $l$  tends to infinity. Studying the linearized system one shows that  $\tilde{\psi} = 0 + 2k\pi$  is a stable equilibrium, and  $\tilde{\psi} = \pi + 2k\pi$  is unstable (repulsive). Thus, except if  $\tilde{\psi}(0) = \pi + 2k\pi$ , one gets  $\tilde{\psi} \rightarrow 0$ . Linearizing around 0, it is straightforward that the convergence is exponential.

It is proved in Lemma 2, that  $\epsilon \leq \tilde{s} \leq A$  (the result is still valid under the assumptions of the present theorem as it does not depend on the behavior of  $\tilde{\psi}$ ). Thus there is no peaking. As soon as  $\tilde{\psi}$  has converged, the exponential convergence of the rest the error system is thus straightforward in the time scale  $dl$ , as  $d\tilde{s}/dl = -(k_s \tilde{s}) \tilde{s} \leq -k_s \epsilon \tilde{s}$ . Indeed, considering  $\tilde{s}^2$  as a Lyapunov function for the rest of the system, one has

$$d\frac{\tilde{s}^2}{dl}(\tilde{s})^2 \leq -2k_s \epsilon (\tilde{s})^2,$$

which proves exponential convergence.  $\square$

## References

- Abuhadrous, I., Ammoun, S., Nashashibi, F., Goulette, F., & Lurgeau, C. (2004). Digitizing and 3D modeling of urban environments and roads using vehicle-borne laser scanner system. In *Proceedings of the 2004 IEEE/RSJ international conference on intelligent robots and systems* (pp. 76–81).
- Barber, D., Mills, J., & Smith-Voysey, S. (2008). Geometric validation of a ground-based mobile laser scanning system. *ISPRS Journal of Photogrammetry and Remote Sensing*, 63, 128–141.
- Bevly, D. (2004). Global positioning system (GPS): A low-cost velocity sensor for correcting inertial sensor errors on ground vehicles. *Journal of Dynamic Systems, Measurement and Control*, 126, 255–264.
- Bevly, D., Ryu, J., & Gerdes, J. (2006). Integrating INS sensors with GPS measurements for continuous estimation of vehicle sideslip, roll, and tire cornering stiffness. *IEEE Transactions on Intelligent Transportation Systems*, 7, 483–493.
- Bonnabel, S., Martin, P., & Rouchon, P. (2008). Symmetry-preserving observers. *IEEE Transactions on Automatic Control*, 53, 2514–2526.
- Bonnabel, S., Martin, P., & Rouchon, P. (2009). Non-linear symmetry-preserving observers on Lie groups. *IEEE Transactions on Automatic Control*, 54, 1709–1713.
- Davidson, P., Hautamäki, J., & Collin, J. (2008). Using low-cost mems 3d accelerometers and one gyro to assist gps based car navigation system. In *Proceedings of the 15th international conference on integrated navigation systems*.
- Di Domenico, D., Fiengo, G., & Glielmo, L. (2007). On-board Prototype of a vehicle localization system. In *IEEE international conference on control applications* (pp. 438–443).
- Dissanayake, G., Sukkarieh, S., Nebot, E., & Durrant-Whyte, H. (2001). The aiding of a low-cost strapdown inertial measurement unit using vehicle model constraints for land vehicle applications. *IEEE Transactions on Robotics and Automation*, 17, 731–747.
- Fiengo, G., Di Domenico, D., & Glielmo, L. (2009). A hybrid procedure strategy for vehicle localization system: Design and prototyping. *Control Engineering Practice*, 17, 14–25.
- Grip, H., Imsländ, L., Johansen, T., Fossen, T., Kalkkuhl, J., & Suissa, A. (2008). Nonlinear vehicle side-slip estimation with friction adaptation. *Automatica*, 44, 611–622.
- Guillaume, D., & Rouchon, P. (1998). Observation and control of a simplified car. In *Proceedings of the 1998 IFAC international workshop on motion control* (pp. 63–67).
- Hamel, T., & Mahony, R. (2006). Attitude estimation on  $SO(3)$  based on direct inertial measurements. In *Proceedings of the 2006 IEEE international conference on robotics and automation* (pp. 2170–2175).
- Hohman, D., Murdock, T., Westerfield, E., Hattox, T., & Kusterer, T. (2000). GPS roadside integrated precision positioning system. In *Position location and navigation symposium* (pp. 221–230).
- Ignatyev, A. (1997). Stability of a linear oscillator with variable parameters. *Electronic Journal of Differential Equations*, 1–6.
- Imsländ, L., Johansen, T., Fossen, T., Fjær Grip, H., Kalkkuhl, J., & Suissa, A. (2006). Vehicle velocity estimation using nonlinear observers. *Automatica*, 42, 2091–2103.
- Lageman, C., Mahony, R., & Trumpf, J. (2008). State observers for invariant dynamics on a Lie group. In *Proceedings of the international conference on the mathematical theory of networks and systems*.
- Lageman, C., Trumpf, J., & Mahony, R. (2010). Gradient-like observers for invariant dynamics on a Lie group. *IEEE Transactions on Automatic Control*, 55, 367–377.
- Mahony, R., Hamel, T., & Pfimlin, J.-M. (2008). Nonlinear complementary filters on the special orthogonal group. *IEEE Transactions on Automatic Control*, 53, 1203–1218.
- Martin, P., & Salaün, E. (2007). Invariant observers for attitude and heading estimation from low-cost inertial and magnetic sensors. In *Proceedings of the 46th IEEE conference on decision and control* (pp. 1039–1045).
- Martin, P., & Salaün, E. (2008a). A general symmetry-preserving observer for aided attitude heading reference systems. In *Proceedings of the 47th IEEE conference on decision and control* (pp. 2294–2301).
- Martin, P., & Salaün, E. (2008b). An invariant observer for Earth-velocity-aided attitude heading reference systems. In *Proceedings of the 17th IFAC world congress* (pp. 9857–9864).
- Martin, P., & Salaün, E. (2010). Design and implementation of a low-cost observer-based attitude and heading reference system. *Control Engineering Practice*, 18, 712–722.
- Nagrath, L., & Gopal, M. (2006). *Control systems engineering*. New Age International Publisher.
- Ryu, J., & Gerdes, J. (2004). Integrating inertial sensors with global positioning system (GPS) for vehicle dynamics control. *Journal of Dynamic Systems, Measurement, and Control*, 126, 243–254.
- Sebsadji, Y., Glaser, S., Mammar, S., & Dakhllallah, J. (2008). Road slope and vehicle dynamics estimation. In *Proceedings of the American control conference* (pp. 4603–4608).
- Vasconcelos, J., Cunha, R., Silvestre, C., & Oliveira, P. (2007). Landmark based nonlinear observer for rigid body attitude and position estimation. In *Proceedings of the 46th IEEE conference on decision and control* (pp. 1033–1038).
- Vasconcelos, J., Silvestre, C., & Oliveira, P. (2008). A nonlinear GPS/IMU based observer for rigid body attitude and position estimation. In *Proceedings of the 47th IEEE conference on decision and control* (pp. 1255–1260).
- Zhang, P., Gu, J., Milios, E., & Huynh, P. (2005). Navigation with IMU/GPS/digital compass with unscented Kalman filter. In *Proceedings of the IEEE international conference on mechatronics & automation* (pp. 1497–1502).